

Vertical flow immunoassay based on carbon black nanoparticles for the detection of IgG against SARS-CoV-2 Spike-protein in human serum: proof-of-concept

Maria Kropaneva,^{*a,b} Pavel Khramtsov,^{a,b} Maria Bochkova,^{a,b} Sergey Lazarev,^{a,b} Dmitriy Kiselkov,^c and Mikhail Rayev^{a,b}

Abstract

Point-of-care tests play an important role in serological diagnostics of infectious diseases and post-vaccination immunity monitoring, including COVID-19. Currently, lateral flow tests dominate in this area and show good analytical performance. However, studies to improve the effectiveness of such tests remain important. In comparison with lateral flow tests, vertical flow immunoassays allow for a reduction in assay duration and the influence of the hook effect. Additionally, the use of carbon black nanoparticles (CNP) as a color label can provide a lower detection limit (LOD) compared to conventional colloidal gold. Therefore, we have developed a vertical flow immunoassay for the detection of IgG against SARS-CoV-2 Spike-protein in human serum samples by applying a conjugate of CNP with anti-human IgG mouse monoclonal antibodies (CNP@MAb). The vertical flow assay device consists of a plastic cassette with a hole on its top containing a nitrocellulose membrane coated with Spike-protein and an absorbent pad. The serum sample, washing buffer, and CNP@MAb flow vertically through the nitrocellulose membrane and absorbent pads, reducing the assay time and simplifying the procedure. In positive samples, the interaction of CNP@MAb with anti-spike antibodies leads to the appearance of black spots, which can be visually detected. The developed method allows for rapid visual detection (5-7 minutes) of IgG vs Spike-protein with a LOD of 7.81 BAU/mL. It has been shown that an untrained operator can perform the assay and visually evaluate its results. Thus, the presented assay can be used in the further development of test systems for the serological diagnostics of COVID-19 or post-vaccination immunity monitoring.

Introduction

The pandemic associated with the novel beta-coronavirus (β -CoV or Beta-CoVs), severe acute respiratory syndrome coronavirus 2 (SARS-CoV-2), which caused the 2019 outbreak of coronavirus disease (COVID-19), has become a major public health problem.¹ This has led to the rise of many studies devoted to the development of test systems for the serological diagnostics of COVID-19 and post-vaccination immunity monitoring.^{2,3} However, the development of point-of-care tests for limited resource settings still remains important.⁴ Such assays should be easy to use, stable during storage, and available for large-scale production. Currently, lateral flow tests dominate in this area, showing high sensitivity and

specificity, which can reach 97-99%.⁵ Despite this, lateral flow assays from a number of manufacturers did not show sufficient effectiveness, and their production and sales were suspended by regulators.⁶⁻⁸

Vertical flow immunoassay (VFIA), also known as immunofiltration or flow-through immunoassay, is a point-of-care test that consists of a matchbox-sized plastic cassette containing an absorbent pad and a porous nitrocellulose membrane on its top. The plastic lid of the cassette has an injection hole which is used for the addition of samples and reagents. Capture and recognition of the analyte occur on the surface of the nitrocellulose membrane, while excess reagents pass through the membrane into the absorbent pad (Fig. 1A). The application of colored labels, usually colloidal gold, allows for visual detection of the analyte (Fig. 1B, C, D), although scanners or cameras can be used to obtain quantitative results.

^a Institute of Ecology and Genetics of Microorganisms, UrB of RAS, Perm, Russia.
E-mail: kropanevamasha@gmail.com.

^b Biology faculty, Perm State University, Perm, Russia

^c Institute of Technical Chemistry, UrB of RAS, 614013 Perm, Russia.

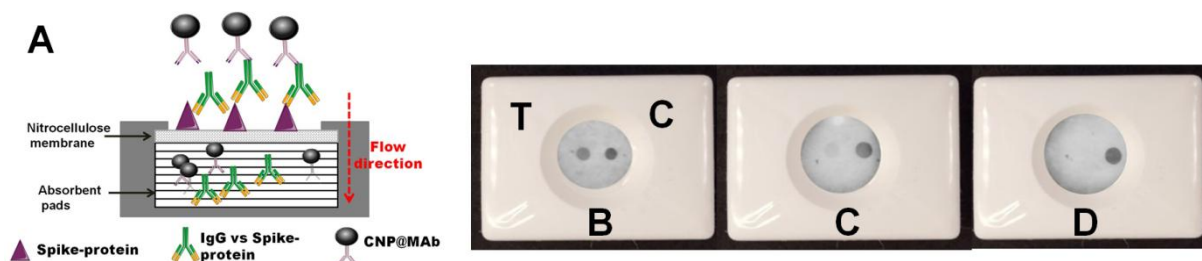


Fig.1. A) Scheme of VFIA for IgG vs Spike-protein detection. Examples of VFIA results. B) VFIA results of serum sample with high IgG vs Spike-protein level; C) VFIA results of serum sample with middle IgG vs Spike-protein level; D) VFIA results of serum sample with low IgG vs Spike-protein level or negative serum sample. C-control; T-test.

Vertical flow immunoassay is used for the detection of biomarkers,^{9,10} antibodies,¹¹⁻¹³ pathogenic organisms,¹⁴⁻¹⁵ and antibiotics.¹⁶ It is worth mentioning that the Canadian = company bioLytical® Laboratories produces a test for the determination of antibodies against HIV in a flow-through format.¹⁷ The test was approved by the WHO and the FDA. In comparison with lateral flow tests, VFIA allows for a reduction in assay time and the elimination of a hook effect, as demonstrated by Oh and co-authors.¹⁸⁻²⁰ The most frequently utilized labels in VFIA are colloidal gold^{11,12,15,20-23} and horseradish peroxidase.^{14,24} Quantum dots⁹ and colloidal dyes²⁵ can also be used as labels.

Colloidal carbon, as a colored label, provides numerous advantages in the development of colorimetric assays. Carbon black conjugates are intensely colored, allowing for a high level of analytical signal and a high signal-to-noise ratio, which can significantly decrease the limit of detection. For example, Porras and co-authors have demonstrated that carbon nanoparticles (CNPs) provide a higher sensitivity (3.8 times) compared to gold nanoparticles in the lateral flow test for nucleic acids detection.²⁶ The details of CNPs usage in immunoassays are discussed in-depth in the following works.²⁷⁻³⁰ Moreover, carbon black is a widely used and inexpensive material, with a standardized production process and properties. A number of research groups have taken advantage of CNPs for the development of paper-based and lateral flow tests.³¹⁻³⁴ Thus, the application of carbon nanoparticles conjugate in VFIA is a promising option.

Herein, we have developed, for the first time, a vertical flow immunoassay based on carbon black nanoparticles for the detection of immunoglobulin G against the Spike-protein of SARS-CoV-2. The immunoassay involves several simple steps and can be performed in modern laboratories by untrained operators (CV for intra-operator precision does not exceed 15%). The detection limit of the assay is 7.81 BAU/mL. Visual

detection of IgG vs the Spike-protein in a single serum sample can be assessed within 5-7 minutes. The work also presents and discusses the methodological aspects of the developed assay.

Experimental

Materials

Streptavidin was from ProspecBio (Israel). Tween-20 was from ITW (USA). Mouse monoclonal IgG2a against human IgG further designated as MAb and recombinant spike protein of SARS-CoV-2 were obtained from HyTest (Finland). Human IgG from human serum and Casein was from Sigma-Aldrich (USA). Bovine serum albumin was from Biosera (France). Biotinylation of BSA was performed as described in [Harlow, 1999].

Samples of different carbon black types (N115, N231, N326, N330, N772, P803) were kindly provided by A. L. Gabov (Perm State University, Russia; Chemical faculty, department of physical chemistry) as a dry powder.

Instrumentation. Multiskan Sky UV-Vis Reader was from Thermo Scientific (USA). ZetaSizer NanoZS particle analyzer was from Malvern (UK). VCX-130 ultrasonic processor was from Sonics & Materials (USA). Scanning electron microscope FEI Quanta 650FEG (Thermo, USA).

Components of devices for vertical flow immunoassay: nitrocellulose membranes (CLW-040, 0.3 μm /0.45 μm /0.8 μm), absorbent pad AP-080 and plastic cases were from Advanced Microdevices Pvt. Ltd (MDI) (India).

Buffers for preparation of carbon black nanoparticles conjugates:

Borate buffer pH 8.8 (BB) was prepared by adjusting 50 or 100 mM H3BO3 solutions (Sigma-Aldrich, USA) to the desired pH with 0.1 M NaOH (Panreac, USA). Coupling buffer : 50 mM BB; Washing buffer : 50 mM BB + 1 % (w/v) BSA; Storage buffer:

100 mM BB + 1 % (w/v) BSA + 0.53 % ProClin950 (0.05 % 2-Methyl-4-isothiazolin-3-on) (Sigma-Aldrich, USA).

Buffers for vertical flow immunoassay:

0.01 M Phosphate-buffered saline (PBS): 0.137 mol/L NaCl + 0.0027 mol/L KCl, pH 7.4 (Ecoservice, Russia) + 0.53 % ProClin950. Coating buffer: PBS; Washing buffer: PBS + 0.1 % Tween-20; Blocking buffer: PBS + 0.4 % Tween-20.

All buffers were prepared using deionized water.

Methods

Conjugation of CNP with anti-human MAb and Bi-BSA. Carbon black nanoparticles (CNP) were conjugated with MAb or Bi-BSA according to the method described in [Van Amerongen, 1993; O'Keeffe, 2003], with modifications. CNP was diluted to the final concentration 2 mg/mL with 1 mL of coupling buffer and ultrasonicated on the ice bath (probe diameter — 3 mm; amplification — 60 %; duration — 1 min). Then, the required amount of Bi-BSA or MAb was added, and ultrasonicated again (probe diameter — 3 mm; amplification — 60 %; duration — 1 min). After incubation for 60 minutes at 37 °C on a rotary mixer (10 rpm), BSA was added to the final concentration of 2 % and incubated (1 hour, 37 °C, rotary mixer). After this stage, the absorbance at 450 nm of obtained suspensions was measured and used to assess nanoparticles concentration at the following synthesis stages. Next, the resulting suspensions CNP@MAb or CNP@Bi-BSA were precipitated by centrifugation at 20,000 g for 30 minutes, the resulting pellets were resuspended in washing buffer, briefly sonicated (10 sec, 60 %) and centrifuged at 20,000 g, 15 minutes. After the third wash cycle, the resulting pellets were resuspended in a 0.5 mL storage buffer and ultrasonicated using a probe sonicator on the ice bath (probe diameter — 3 mm; amplification — 60 %; duration — 1 min). The conjugates were stored at 4 °C and briefly sonicated before usage.

CNP conjugates characterization. The size and monodispersity of nanoparticles were measured by dynamic light scattering (DLS). For this, nanoparticles were diluted 1:350 in deionized water.

To assess the absorbance at 450 nm of the carbon black nanoparticles, obtained suspensions were diluted 1:101 in the washing buffer (10 µl of particles + 1000 washing buffer) in glass cuvette.

For obtaining the SEM images of nanoparticles CNP conjugate samples were dropped onto silicon wafers (5 × 5 mm), dried overnight at room temperature, and analyzed by SEM.

Fabrication of nitrocellulose immunosorbent. The nitrocellulose membrane was coated with Spike-protein (2 µl per dot) diluted in coating buffer and dried (30 min RT, 90 min 37 °C in a drying oven). Next, the immunosorbent was transferred to the plate and washed by 30 mL of washing buffer for 5 minutes 3 times. After that, the membrane was incubated with 35 mL of blocking buffer (60 min, 37 °C) for elimination of the non-specific interactions. Then washing procedure was repeated.

After that immunosorbent was dried (30 min RT, 90 min at 37 °C in drying oven), cut into small strips (15 mm and 15 mm) and placed over 10 stacks of absorbent pads supported on a solid plastic case. Further, the presented device was closed by a lid with a hole for the sample addition (Figure S1†).

Assay procedure. The reagents were dropped onto the immunosorbent sequentially. Initially, 150 µl of washing buffer was dropped onto the immunosorbent to the full absorption of liquid, followed by 100 µl of test sera in blocking buffer (Fig. 2A). After the 1 minute incubation and second wash cycle, 80 µl of CNP@MAb was added to visualize the spot on the immunosorbent and incubated for 1 minute (Fig. 2B). Assay results were analyzed after the third wash cycle with 200 µl of washing buffer (Fig. 2C). For optimization experiments the images of the immunosorbent were processed in the ImageJ software, according to the method described in the article.³⁵ Detailed description is given in Supplementary materials (Fig. S4†).



Fig. 2. Vertical flow assay procedure. A) Addition of analyzed sample; B) Addition of CNP@ MAb; C) Addition of 200 µl washing buffer. Spike-protein concentration: 1) 0.5 mg/mL; 2) 0.25 mg/mL; 3) 0.125 mg/mL; 4) 0.0625 mg/mL.

Assay parameters for Streptavidin direct detection. The nitrocellulose membrane coated with streptavidin in the four concentrations (0.5, 0.25, 0.12, 0.06 mg/mL) was firstly dried and washed. Next, the membrane was dipped into a reservoir with a blocking buffer and incubated for 1 hour, 37 °C. After washing and drying, prepared nitrocellulose membrane was used in VFIA for streptavidin detection. Analytical signal was obtained by CNP@BSA-Bi diluted to the final concentration 0.25 mg/mL in the blocking buffer (Fig. 3A).

Assay parameters for indirect detection of IgG vs Spike-protein. Spike-protein was sorbed onto the nitrocellulose membrane in the final concentration 0.25 mg/mL, analyzed serum samples were dissolved 1/10 in the blocking buffer. 0.25 mg/mL CNP@MAb in the blocking solution was used for analytical signal obtaining (Fig. 1A).

Clinical serum samples. Human serum samples from patients with verified diagnosis of a new coronavirus infection (Covid-19) were obtained from Clinical industrial hospital №1, Perm Krai, Russia. Due to the widespread of the new coronavirus infection and vaccination, obtaining negative serum samples is problematic. Therefore, serum samples obtained before 2019 were used as negative samples. All clinical samples were firstly analyzed and the levels of immunoglobulin against SARS-CoV-2 Spike-protein (IgG vs Spike-protein) were measured using

commercial ELISA kit (Vector-Best, Russia, www.vector-best.ru). The test was performed according to the manufacturer's instructions. As a result a positive blood sera with various concentrations of IgG vs Spike-protein were collected. Samples obtained before 2019 according to the results of the ELISA were determined as negative. Additionally, positive and negative serum pools were prepared by mixing 3 positive serum samples and 10 negative serum samples, respectively. Preserving agent Proclin 950 was added in each pool to the final concentration of 0.53 %. Concentration of IgG vs Spike-protein in the positive serum pool was 5536.2 BAU/mL and 0 BAU/mL in the negative serum pool, according to ELISA.

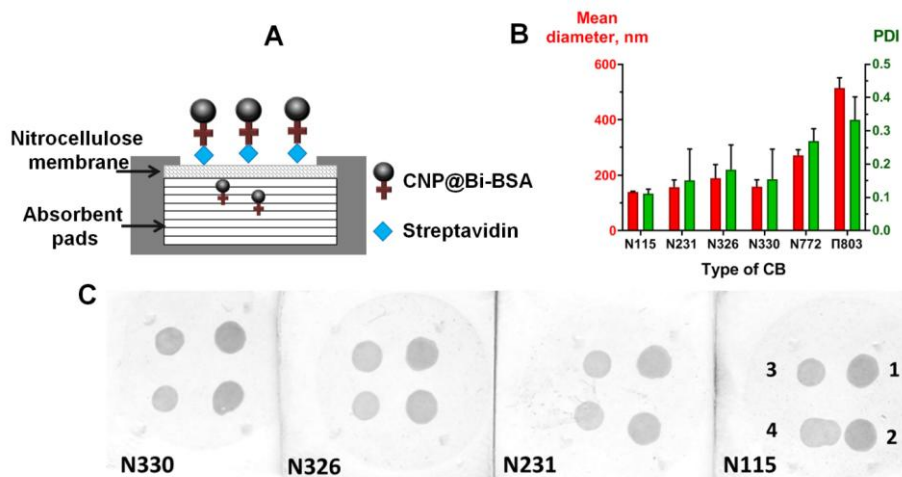
This research was performed according to World Medical Association's Declaration of Helsinki and Council of Europe Protocol to the Convention on Human Rights and Biomedicine and approved by the Ethics Committee of the Institute of Ecology and Genetics of Microorganisms, Ural Branch of the Russian Academy of Sciences (IRB00010009). Written informed consent was obtained from all the participants.

Results and discussion

Optimization of CNP conjugates preparation.

Carbon black type optimization. Different types of carbon black have a wide range of primary particle sizes, surface area per

immunoassay development, particle size and surface characteristics contribute to tinting strength, blackness, and the protein adsorption process.³⁶ These parameters can ultimately affect the specificity and sensitivity of the immunoassay, as well as the stability of the conjugate.³⁷ In this series of experiments, for reasons of economy, CNPs were functionalized with Bi-BSA (CNP@Bi-BSA) rather than with monoclonal antibodies. We obtained CNP@Bi-BSA based on six types of carbon black: N115, N231, N326, N330, N772, and P803. The size and polydispersity of these CNP@Bi-BSA, as well as their performance in a model VFIA for direct streptavidin detection (Fig. 3A), were measured. As expected, the type of carbon black affected the size of the conjugates. The application of carbon black N115 provided CNP@Bi-BSA with the smallest diameter of 139.9 ± 1.63 nm and a polydispersity index of 0.11 ± 0.01 (Fig. 3C). Carbon blacks N772 and P803 yielded very large conjugates that could not pass through the membrane and were excluded from the further comparative analysis. For the other CNP@Bi-BSA, the diameters and PDI were in the range of 157-188 and 0.11-0.11, respectively. It was shown that the functional activity of CNP conjugates didn't depend on the type (N115, N231, N326, N330) of carbon black (Fig. 3B). In the further studies, carbon black N115 was used, because it has the lowest size and polydispersity.



unit mass, and degrees of particle aggregation. In terms of

Fig. 3. A) Scheme of VFIA for direct streptavidin detection; Results of carbon black type optimization: B) Mean diameter and polydispersity of the obtained CNP@Bi-BSA. (PDI-polydispersity index; the vertical bars indicate the standard deviation, $n = 3$); C) Functional activity of the obtained CNP@Bi-BSA (Streptavidin concentration, mg/mL: 1-1, 2-0.5, 3-0.25, 4-0.125

The optimal amount of MAb. We conjugated CNP with MAb in ratios ranging from 10 to 250 μ g of MAb per 1 mg of CNP and compared the obtained CNP@MAb in the vertical flow immunoassay of IgG vs Spike-protein (Fig. 1A). The conjugate of CNP with bovine serum albumin in the ratio 250:1 was used as a negative control.

The vertical flow assay was performed using a pool of positive sera (5536.2 BAU/mL) and negative sera (0 BAU/mL). After the completion of the assay, the membranes were removed, dried, scanned, and the obtained images were processed in ImageJ software. The analytical signal increased as the MAb-to-CNP ratio increased (Fig. 4A, B), and a substantial increment of the signal was observed from the ratio of 100:1 to the ratio of

150:1. No colored spots were observed in the negative samples and for the control conjugate.

The performance of the four best CNP@MAb conjugates (with MAb-to-CNP ratios from 150:1 to 250:1) was compared using 10-fold dilutions of the positive pool. The final concentration of IgG vs Spike-protein in the diluted samples was 0.55, 5.54, 55.4, and 553.6 BAU/mL. The pool of negative sera was used as a zero sample. The highest signal was obtained when the MAb-to-CNP ratios were 200:1 and 250:1 (Fig. 4C).

The amount of protein on the CNP surface can affect its size and polydispersity. Insufficient protein coating can decrease

the stability of the conjugates and, accordingly, the efficiency of the assay.³⁸⁻⁴¹ According to DLS, the mean diameter of the obtained CNP@MAb was 150-170 nm (Fig. 4D). SEM images showed that the nanoparticles had a spherical shape (Fig. S2†). The size of the CNP@MAb was approximately the same for all MAb-to-CNP ratios and did not change for 2 months at 4 °C (Fig. 4D). Thus, the MAb-to-CNP ratio of 10:1 is sufficient to maintain the colloidal stability of the obtained nanoparticles. However, from the point of view of VFIA development, a ratio of 200 µg and above of MAb per 1 mg of CNP is optimal.

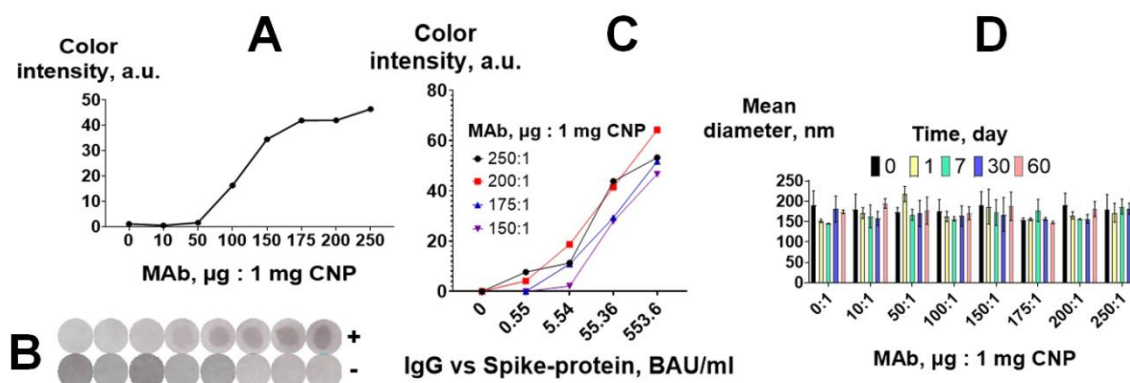


Fig. 4. Optimization of CNP@MAb preparation. A) Analytical signal of VFIA for positive serum pool; B) Visual assessment of VFIA for positive (+) and negative (-) serum pool; C) Calibration curves of IgG vs Spike-protein obtained in VFIA; D) Colloidal stability of CNP@MAb conjugates (Mean±SD, n = 3)

Reproducibility of CNP@MAb preparation. The reproducibility of nanoparticle conjugate synthesis is essential for its further practical application. To assess the reproducibility of the functionalization, three batches of CNP@MAb were prepared. VFIA for IgG vs Spike-protein determination was constructed using positive pooled serum diluted tenfold in blocking buffer,

and negative pooled serum was used as a zero sample for the assessment of CNP@MAb functional activity. Human IgG and Spike-protein at a concentration of 0.25 mg/mL were dotted in the control and test zone, respectively. The results are shown in Table S1† and Figure 5. Nanoparticles with similar sizes (183-184 nm), polydispersity (0.17-0.19), concentrations (3.3-4.2), and functional activities were obtained.

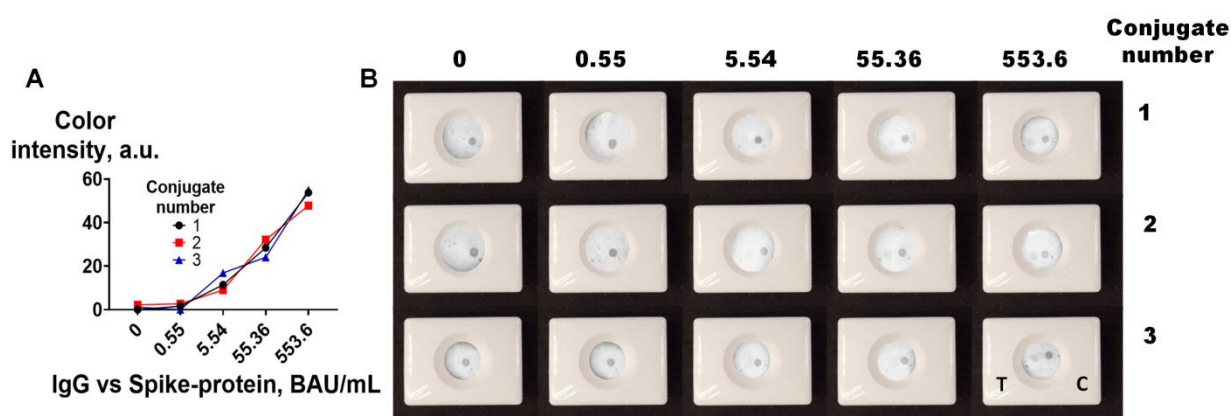


Fig. 5. Reproducibility of CNP functionalization: A) Results obtained by scanner and ImageJ processing. B) Visual assessment of VFIA. T-test; C-control.

Optimization of vertical flow immunoassay.

Membrane type optimization. It is known that the pore size of the nitrocellulose membrane can affect the results of solid phase immunoassay. For example, a small pore size provides a larger surface area and a greater number of antigen-binding sites, resulting in lower limits of detection.⁴² Nitrocellulose membranes with pore sizes of 0.3, 0.45, and 0.8 μm were tested in the model VFIA for streptavidin detection (Fig. 3A). A pore size of 0.3 μm provides a high analytical signal, low background, and uniformly colored spots (Fig. 6).

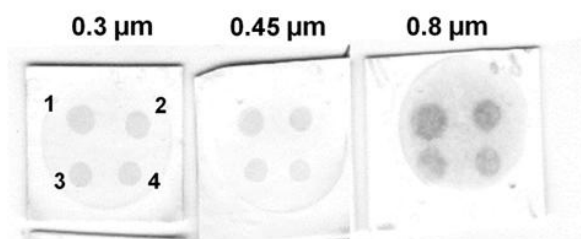


Fig. 6. Influence of the nitrocellulose membrane pore size on the results of model VFIA based on CNP@Bi-BSA. Streptavidin concentration: 1) 1 mg/mL; 2) 0.5 mg/mL; 3) 0.25 mg/mL; 4) 0.125 mg/mL.

Optimal blocking solution. The purpose of blocking a nitrocellulose membrane is to prevent nonspecific interactions between assay components. Blocking also serves other functions, including the maintenance of membrane hydration, modification of wicking rates, and stabilization of adsorbed

proteins.^{43,44} The concentration and type of blocking agent are usually determined empirically for compatibility with the specific sample and antibody-antigen system.

The effect of the following common blocking agents (casein, BSA, and detergent Tween-20)^{44,45} at three different concentrations was assessed by detecting IgG vs Spike-protein. Figures 7B and C show that Tween-20 at a concentration of 0.4% provides the highest signal and low background. It should be noted that the level of the background signal was lower when casein was used (Fig. 7C). This could affect the assay results, especially for samples with low antibody levels. Therefore, the influence of the three best blocking solutions on the calibration curves in the IgG vs Spike-protein assay was studied. Tween-20 at a concentration of 0.4% provides better detection limits (the color of the test zone for an antibody concentration of 0.55 BAU/mL could be distinguished from the color of the test zone without antibodies) (Fig. 7A). In further studies, 0.4% Tween-20 was used for blocking and dilution of the analyzed samples and the detection reagent.

Optimal concentrations of Spike-protein and CNP@MAb. Spike-protein was adsorbed on a nitrocellulose membrane at concentrations of 0.5, 0.25, 0.125, and 0.0625 mg/mL. Tenfold dilutions of the positive sera pool were analyzed. Bound IgG vs Spike-protein was detected using four concentrations of CNP@MAb: 0.25, 0.17, 0.1, and 0.07 mg/mL. Figure 8 shows that a concentration of 0.25 mg/mL is optimal for both Spike-protein and CNP@MAb. A reduction in the concentration of both the Spike-protein and CNP@MAb leads to a significant decrease in the analytical signal in samples with low antibody levels (0.55 and 5.54 BAU/mL).

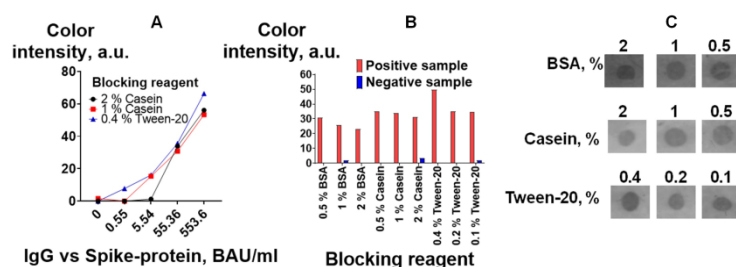


Fig. 7. Optimization of blocking buffer A) Calibration curves for the determination of IgG vs Spike-protein by the VFIA; Analytical signal of vertical flow-through assay: results of image analysis with software ImageJ (B) and visual assessment of positive samples (C)

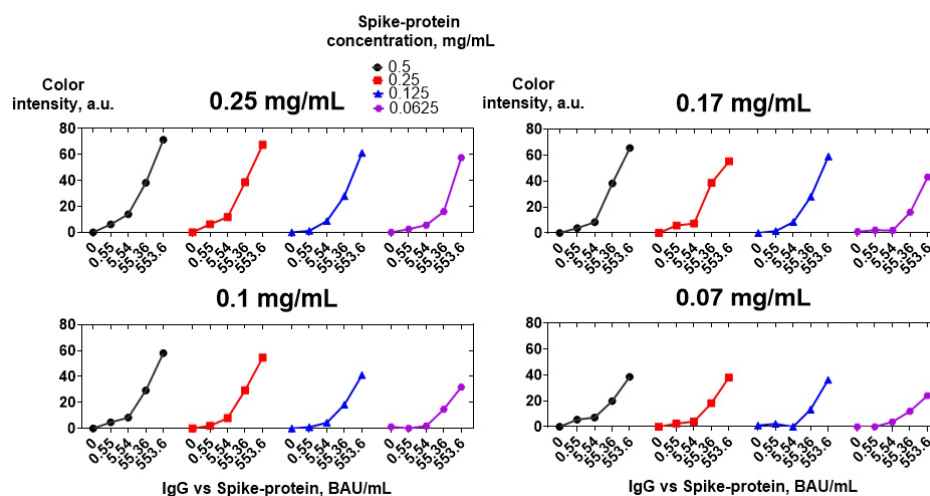


Fig.8. Optimization of Spike-protein and CNP@MAb concentrations. Concentrations of CNP@MAb are specified above the graphs.

Optimization of an assay procedure. The volume of the CNP@MAb and washing buffer at the last stage of the assay (washing step after incubation with CNP@MAb) was optimized. The optimal volume of CNP@MAb was found to be 80 μ l. Increasing the volume of the detection reagent to 320 μ l did not significantly affect the analytical signal of samples with low antibody levels (0.55 BAU/mL) (Fig. 9B). The volume of the washing buffer also did not affect the assay results (Fig. 9A).

Assay validation.

VFIA for IgG vs Spike-protein detection was constructed under optimal experimental conditions using negative pooled serum diluted tenfold in blocking buffer as a diluent for analyzed samples. Human IgG and Spike-protein at a concentration of 0.25 mg/mL were dotted in the control and test zone, respectively. It can be seen that when the concentration of IgG vs Spike-protein is 7.81 BAU/mL or higher, the color of the test zone can be distinguished from the background (Fig. 10). Thus, the limit of detection (LOD) of the presented VFIA was determined to be 7.81 BAU/mL. Taking into account that during the VFIA process, the analyzed sample is diluted 1/10, the developed vertical flow carbon black immunoassay allows for rapid visual identification of samples with antibody concentrations greater than 78.1 BAU/mL.

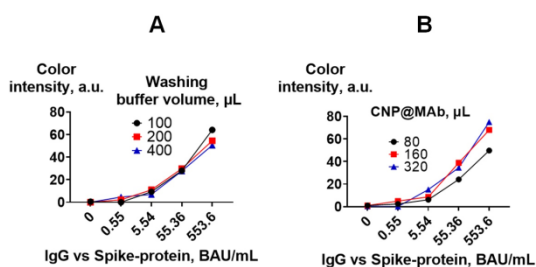


Fig. 9. Optimization of VFIA procedure. Calibration curves for the determination of IgG vs Spike-protein were presented. A) Optimal washing buffer volume; B) Optimal CNP@MAb volume.

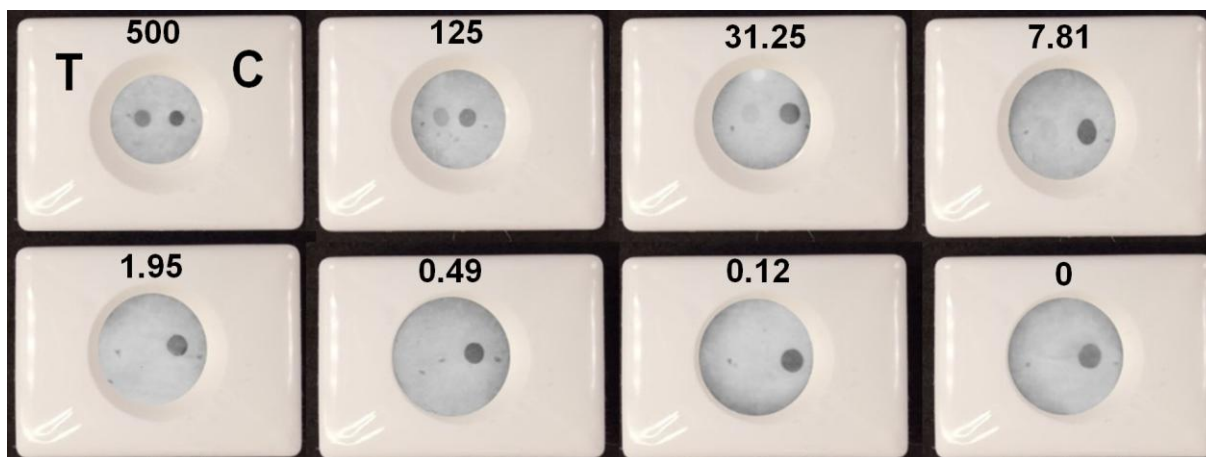


Fig. 10. Determination of IgG vs Spike-protein by the VFIA in optimal conditions. Concentrations of antibodies in BAU/mL are specified above the images.

For the assessment of assay reproducibility, ten serum samples with different concentrations of IgG vs Spike-protein were tested in six replicates. The serum samples were diluted tenfold with a blocking buffer before the assay. Processing the assay results using ImageJ software showed that the coefficients of variation did not exceed 25% for serum samples containing IgG vs Spike-protein in concentrations ranging from 5473.09 to 108 BAU/mL and higher. For negative serum samples and two samples with antibody concentrations lower than 55 BAU/mL, the coefficient of variation exceeded 100%. This high coefficient of variation can be attributed to the measurement of the background intensity, which is relatively non-uniform, rather than the spots.

For the validation of visual assessment, the sensitivity and specificity rates were determined. These parameters are often used to evaluate qualitative analytical methods.⁴⁶ In this study specificity rate indicated the assay ability to determine all 6 replicates of one negative sample as negative. And, respectively, sensitivity rate is the assay ability to determine all 6 replicates of one positive sample as positive. Visual assessment was performed for all 6 replicates of each serum sample. Positive results were marked as 1, and negative results were marked as 0 in Table 1. Then sensitivity and specificity rate were calculated for each serum samples. The values were expressed in percent. We are expected that serum #33 and #48 with concentrations below 55 BAU/mL would be identified as negative, because antibodies concentrations in these samples after dilution are lower than the detection limit. It was confirmed that the specificity rate was 100% for samples

with antibodies below the LOD and two truly negative samples.

It was determined that 5 positive serum samples with antibody concentrations ranging from 5473.09 to 359.3 BAU/mL demonstrated a 100% sensitivity rate. All 6 replicates for these serums were determined as positive. One replicate for sample with antibodies level near the detection limit (#58, 108 BAU/mL) was defined as negative and sensitivity rate was 83%. The evaluation showed that the developed method can determine positive serum as positive with more than 95% reliability for antibody concentrations above 359.3 BAU/mL. The performed VFIA allows for the detection of negative serum as negative with a 100% specificity rate.

Serum sample number	ELISA, BAU/mL	Color intensity, a.u. n=6, Mean \pm standard deviation	CV, %	Detection status for visually assessment						Sensitivity rate, %	Specificity rate, %
				1	1	1	1	1	1		
3	5473.09	49 \pm 3	6.1	1	1	1	1	1	1	100	0
63	2321.8	56.6 \pm 3.7	6.5	1	1	1	1	1	1	100	0
36	1465.6	31.9 \pm 2.6	8.1	1	1	1	1	1	1	100	0
83	564.9	21.6 \pm 4.9	22.7	1	1	1	1	1	1	100	0
61	359.3	10.3 \pm 1.6	15.1	1	1	1	1	1	1	100	0
58	108.0	11.7 \pm 2.4	20.2	0	1	1	1	1	1	83	0
33	54.4	1.6 \pm 2.3	145.8	0	0	0	0	0	0	0	100
48	20.4	0.4 \pm 0.9	223.6	0	0	0	0	0	0	0	100
71	0	0.9 \pm 1.9	223.6	0	0	0	0	0	0	0	100
75	0	2 \pm 1.7	79.2	0	0	0	0	0	0	0	100

Table 1. Assay reproducibility, specificity and sensitivity rate.

To determine inter-operator precision, two blood serum samples (negative and high positive) were analyzed by eight different operators using the optimized VFIA. The operators had various levels of experience in assay performance and were not aware of the sample status. Each operator received written step-by-step instructions for the VFIA procedure, as well as tubes with samples, diluents, conjugate, and washing buffer. The assay results were visually assessed according to the following scheme: two spots - the result is positive (1), one spot in the control zone - the result is negative (0), one spot in the test zone or no spots - the test is invalid (Fig. S3⁺). Additionally, the results of the assay were processed with Image J software.

All operators rated the result of the positive serum sample analysis as positive Fig. 11. The coefficient of variation for

positive results, as assessed with Image J software, was 10.44%, which is within acceptable limits (Table S2⁺).⁴⁷ Eight operators rated the result of the negative serum sample analysis as negative, but one operator (Fig. 11, cassette 9) rated the negative sample as positive. This false-positive result was confirmed by the analysis of the membrane with Image J software. This could be due to an error during the assay procedure, as the operator was unsure if they changed pipette tips when applying positive and negative samples. It should also be noted that another operator (Fig. 11, cassette 14) had doubts about the results of the visual assessment of the negative sample. This can be explained by the non-uniform background.

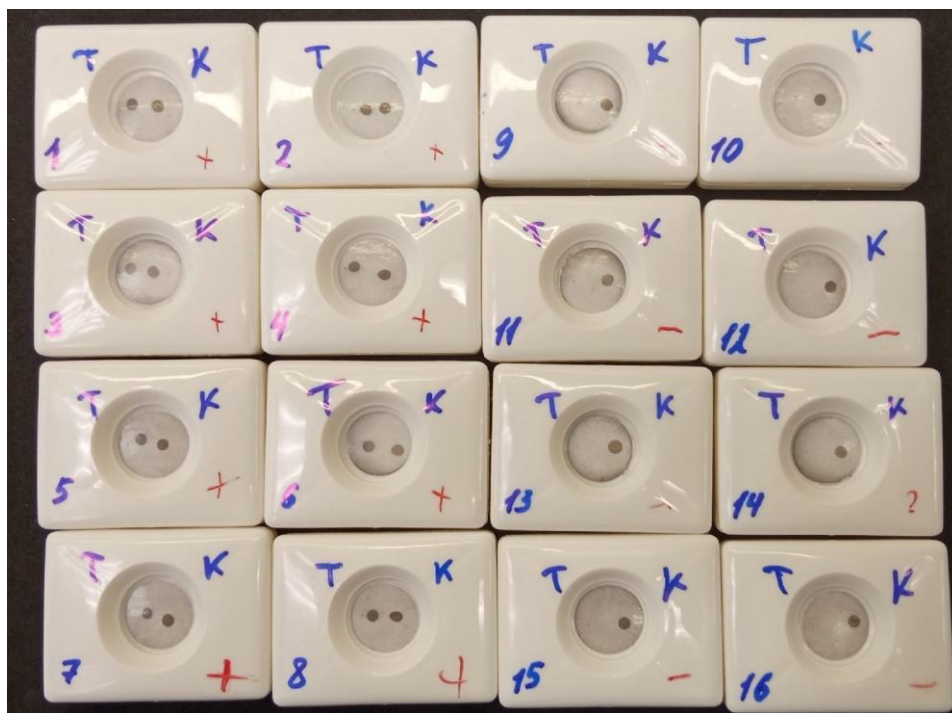


Fig. 11. Inter-operator precision. T-test; K-control (Russian); 1-8 – positive sample; 9-16– negative sample. Each operator performed tests with positive and negative samples: operator 1 - cassettes 1 and 9, operator 2 - cassettes 2 and 10, and so on.

Conclusions

In this study, we have demonstrated, for the first time, the development process of a vertical-flow, nitrocellulose-based immunoassay for the rapid visual qualitative detection of IgG versus Spike-protein in human serum samples using a CNP-based conjugate as a detection reagent. The immunoassay principle demonstrated herein can be applied to create VFIA for the detection of antibodies against various infectious diseases. The optimized assay requires only a few minutes and can be performed by personnel with limited experience in immunoassays. As stated in the title of this paper, we consider this work to be a proof-of-concept study. Determining total IgG against Spike-protein has little clinical significance, as there is no definite protective concentration.⁴⁸ Therefore, we consider the developed immunoassay rather as a platform for the construction of VFIA for neutralizing antibodies, which disrupt the interaction between Spike-protein and the ACE-2 receptor.⁴⁹

Notable result of our study is the successful application of carbon black nanoparticles as labels in VFIA. Previously, only one study reported the use of colloidal carbon in non-instrumental and semi-instrumental flow-through assays.¹⁹ Despite the potential advantages, carbon black remains a less

preferred label in lateral flow and flow-through tests, even though several studies have shown that it outperforms conventional gold nanoparticles.^{26,50,51} We confirmed that commercial carbon black enables the preparation of antibody conjugates in a rapid, simple, and reproducible manner. Considering recent papers that demonstrate lower limits of detection (LODs) for other black-colored nanoparticles in LFIA,⁵² we suggest that researchers should pay more attention to CNP as a commonly available and potentially more efficient alternative to conventional labels in point-of-care tests. At the same time, we identified several shortcomings associated with the use of CNPs. We observed a decrease in the functional activity of the conjugates during long-term storage, which may be due to the desorption of antibodies, both passively and mediated by BSA presented in the storage buffer. The non-uniform background is likely a result of hydrophobic interactions between carbon black nanoparticles and the nitrocellulose membrane. These interactions cannot be completely eliminated, even by coating the nanoparticles with an excess of proteins (IgG and BSA). One potential solution to overcome these disadvantages is the covalent attachment of antibodies⁵⁰ and the hydrophilization of CNP surfaces through polymer coating or chemical treatment.

Author Contributions

Conceptualisation - MK, PK and MR. Methodology, investigation, project administration, visualisation- MK, PK, MB, SL and MR. Supervision-MR. Funding acquisition – MB and SL. Writing original craft - MK and PK. Writing review and editing - MK, PK, MB, SL and MR. Resources – DK.

Conflicts of interest

There are no conflicts to declare

Acknowledgements

This study was supported by the Russian Science Foundation and the Government of Perm krai, grant 22-24-20091.

Notes and references

- 1 Weekly epidemiological update on COVID-19 - 22 June 2023, <https://www.who.int/publications/m/item/weekly-epidemiological-update-on-covid-19---22-june-2023>, (accessed 27.06.2023)
- 2 M. Harun-Ur-Rashid, T. Foyez, I. Jahan, K. Pal and A.B. Imran, *RSC Adv.*, 2022, **12**, 9445-9465.
- 3 S. Iravani, *Mater. Adv.*, 2020, **1**, 3092-3103.
- 4 O. Vandenberg, D. Martiny, O. Rochas, A. van Belkum and Z. Kozlakidis, *Nat. Rev. Microbiol.*, 2021, **19** (3), 171-183.
- 5 L.J. Robertson, J.S. Moore, K. Blighe, K.Y. Ng, N. Quinn, F. Jennings, G. Warnock, P. Sharpe, M. Clarke, K. Maguire, S. Rainey, R.K. Price, W.P. Burns, A.M. Kowalczyk, A. Awuah, S.E. McNamee, G.E. Wallace, D. Hunter, S. Sager, C. Chao Shern, M.A. Nesbit, J.A.D. Mclaughlin and T. Moore, *BMJ Open.*, 2021, DOI: 10.1136/bmjopen-2020-048142.
- 6 E. Ernst, P. Wolfe, C. Stahura and K.A. Edwards, *Talanta*, 2021, DOI: 10.1016/j.talanta.2020.121883.
- 7 B. Pérez-López and M. Mir, *Talanta*, 2021, DOI:10.1016/j.talanta.2020.121898.
- 8 T. Dong, M. Wang, J. Liu, P. Ma, S. Pang, W. Liu and A. Liu, *Chem. Sci.*, 2023, **14**, 6149-6206.
- 9 P. Zhang, Y. Bao, M.S. Draz, H. Lu, C. Liu and H. Han, *Int J Nanomedicine.*, 2015, **10**, 6161-6173.
- 10 A. Rapak and A. Szewczuk, *Eur. J. Clin. Chem. Clin. Biochem.*, 1993, **31**, 153- 157.
- 11 R. Castro, H.C. Mody, S.Y. Parab, M.T. Patel, S.E. Kikkert, M.M. Park and R.C. Ballard, *Sex Transm Infect.*, 2010, **86**(7), 532-536.B.
- 12 B.K. Sil, M.R. Jamiruddin, M.A.Haq, M.U. Khondoker, N. Jahan, S.S. Khandker, T. Ali, M.J. Oishee, T. Kaitsuka, M. Mie, K. Tomizawa, E. Kobatake, M. Haque and N. Adnan, *Int J Nanomedicine.*, 2021, **16**, 4739-4753.
- 13 S. Kim, Y. Hao, E.A. Miller, D.M.Y. Tay, E. Yee, P. Kongsuphol, H. Jia, M. McBee, P.R. Preiser and H.D. Sikes, *ACS Sens.*, 2021, **6**(5), 1891-1898
- 14 B. Adil, K.M. Shankar, B.T. Kumar, R. Patil, A. Ballyaya, K.S. Ramesh, S.R. Poojary, O.V. Byadgi and P. Siryappagouder, *J Vet Sci.*, 2013, **14**(4), 413-419.
- 15 M. Jia, J. Liu, J. Zhang and H. Zhang, *Analyst*, 2019, **144**, 573.
- 16 Z. Zhi, U.J. Meyer, J. Van den Bedem and M. Meusel, *Anal. Chim. Acta.*, 2001, **442**, 207-219.
- 17 INSTI HIV-1 / HIV-2 Antibody Test, <https://www.insti.com/hiv-test/>
- 18 Y.K. Oh, H.A. Joung, S. Kim and M.G. Kim, *Lab Chip.*, 2013, **13**(5), 768-772.
- 19 G.M.S. Ross, G.I. Salentijn and M.W.F. Nielen, *Biosensors (Basel)*, 2019, **9**(4), 143.
- 20 F. Shi, Y. Sun, Y. Wu, M. Zhu, D. Feng, R. Zhang, L. Peng and C. Chen, *J Appl Microbiol.*, 2020, **128**(3), 794-802.
- 21 O. Genç, O. Büyüktanır and N. Yurdusev, *Trop Anim Health Prod.*, 2012, **44**(2), 213-215.
- 22 Kalita, L.M. Chaturvedula, V. Sritharan and S. Gupta, *Nanomedicine*, 2017, **13**(4), 1483-1490.
- 23 C. Zhang, X. Wu, D. Li, J. Hu, D. Wan, Z. Zhang, B.D. Hammock, *Anal Methods.*, 2021, **13**(14), 1757-1765.
- 24 J.V. Samsonova, V.A. Safronova and A.P. Osipov, *Anal. Biochem.*, 2018, **545**, 43-48
- 25 X. Xiang, W. Tianping and T. Zhigang, *J. Immunol. Meth.*, 2003, **280**, 49-57.
- 26 J.C. Porras, M. Bernuz, J. Marfa, A. Pallares-Rusiñol, M. Martí and M.I. Pividori, *Nanomaterials (Basel)*, 2021, DOI: 10.3390/nano11030741.
- 27 A. van Amerongen, J.H. Wichers, L.B. Berendsen, A.J. Timmermans, G.D. Keizer, A.W. van Doorn, A. Bantjes and W.M. van Gelder, *J Biotechnol.*, 1993, **30**(2), 185-95.
- 28 E.M. Linares, L.T. Kubota, J. Michaelis and S. Thalhammer, *J. Immunol. Methods*, 2012, **375**, 264–270.
- 29 X. Ouyang, J. Liu, J. Li and R. Yang, *Chem Commun (Camb.)*, 2012, **48**(1), 88-90.
- 30 B. Liu, L. Wang, B. Tong, Y. Zhang, W. Sheng, M. Pan and S. Wang, *Biosens Bioelectron.*, 2016, **85**, 337–342.
- 31 L. Mujawar, A. Moers, W. Norde and A. van Amerongen, *Anal Bioanal Chem.*, 2013, **405**, 7469–7476.
- 32 P. Noguera, G.A. Posthuma-Trumpie, M. van Tuil, F.J. van der Wal, A. de Boer, A.P. Moers, A. van Amerongen, *Anal Bioanal Chem.*, 2011, **399**(2), 831-838.
- 33 C. Suárez-Pantaleón, J. Wichers, A. Abad-Somovilla, A. van Amerongen and A. Abad-Fuentes, *Biosens Bioelectron.*, 2013, **42**, 170-176.
- 34 X. Zhang, F. Zhao, Y. Sun, T.n Mi, L. Wang, Qi. Li, J. Li, W. Ma, W. Liu, J. Zuo, X. Chu, B. Chen, W. Han and Y. Mao, *Sens. Actuators B: Chem.*, 2020, DOI:10.1016/j.snb.2020.128458.
- 35 P. Khramtsov, M. Bochkova, V. Timganova, S. Zamorina and M. Rayev, *Anal Bioanal Chem.*, 2017, **409**, 3831–3842.
- 36 Carbon Black, Titanium Dioxide, and Talc, <https://monographs.iarc.who.int/wp-content/uploads/2018/06/mono93.pdf>, (accessed 27.09.2022)
- 37 K.E. Sapsford, W. R. Algar, L. Berti, K. B. Gemmill, B. J. Casey, E. Oh, M. H. Stewart and I. L. Medintz, *Chem. Rev.*, 2013, **113**, 1904–2074.
- 38 I. Zare, D. M. Chevrier, A. Cifuentes-Rius, N. Moradi, Y. Xianyu, S. Ghosh, L. Trapiella-Alfonso, Y. Tian, A. Shourangiz-Haghighi, S. Mukherjee and K. Fan, M. R. Hamblin, *Materials Today*, 2021, **66**, 159-193.
- 39 J. Schubert and M. Chanana, *Curr. Med. I Chem.*, 2018, **25**(35), 4553-4586.
- 40 L. Guerrini, R.A. Alvarez-Puebla and N. Pazos-Perez, *Materials*, 2018, DOI: 10.3390/ma11071154.
- 41 G. Ghosh and L. Panicker, *Soft Matter*, 2021, **17**, 3855-3875.
- 42 P. Chen, M. Gates-Hollingsworth, S. Pandit, A. Park, D. Montgomery, D. AuCoin, J. Gu and F. Zenhausern, *Talanta.*, 2019, **191**, 81-88.
- 43 R.C. Wong, H.Y. Tse (eds.), *Lateral Flow Immunoassay*, DOI 10.1007/978-1-59745-240-3_1, Humana Press, New York, NY 2009
- 44 Rapid Lateral Flow Test Strips. Considerations for Product Development, https://www.merckmillipore.com/INTERSHOP/web/WFS/Merck-RU-Site/ru_RU/-/USD/ShowDocument-Pronet?id=201306.1567, (accessed 27.01.2023)
- 45 A. Frutiger, A. Tanno, S. Hwu, R.F. Tiefenauer, Vörös J. and Nakatsuka N. *Chem Rev.*, 2021, **121**(13), 8095-8160.
- 46 E. Trullols, I. Ruisánchez and F. Rius, *Trends Anal. Chem.*, 2004, DOI:10.1016/S0165-9936(04)00201-8.

- 47 Bioanalytical Method Validation, Guidance for Industry, <https://www.fda.gov/regulatory-information/search-fda-guidance-documents/bioanalytical-method-validation-guidance-industry>, (accessed 27.05.2023)
- 48 Considerations for the use of antibody tests for SARSCoV-2 – first update, <https://www.ecdc.europa.eu/sites/default/files/documents/Considerations-for-the-use-of-antibody-tests-for-SARS-CoV2-first-update.pdf>, (accessed 27.05.2023).
- 49 A.C. Walls, Y.J. Park, M.A. Tortorici, A. Wall, A.T. McGuire and D. Veesler, *Cell*, 2020, **181(2)**, 281-292.
- 50 X. Zhang, X. Yu, K. Wen, C. Li, G. Mujtaba Mari, H. Jiang, W. Shi, J. Shen, and Z. Wang, *J. Agric. Food Chem.*, 2017, **36**, 8063-8071.
- 51 B. Liu, L. Wang, B. Tong, Y. Zhang, W. Sheng, M. Pan, and S. Wang, *Biosens. Bioelectron.*, 2016, **85**, 337-342.
- 52 S. C. Razo, A. I. Elovenkova, I. V. Safenkova, N. V. Drenova, Y. A. Varitsev, A. V. Zherdev, and B. B. Dzantiev, *Nanomaterials*, 2021, **12**, 3277.

Supplemental Data

Vertical flow immunoassay based on carbon black nanoparticles for the detection of IgG against SARS-CoV-2 Spike-protein in human serum: proof-of-concept

Maria Kropaneva,^{*a,b} Pavel Khramtsov,^{a,b} Maria Bochkova,^{a,b}
Sergey Lazarev,^{a,b} Dmitriy Kiselkov,^c and Mikhail Rayev^{a,b}

^aInstitute of Ecology and Genetics of Microorganisms, UrB of RAS, Perm, Russia.

^bBiology faculty, Perm State University, Perm, Russia

^cInstitute of Technical Chemistry, UrB of RAS, 614013 Perm, Russia.

*Corresponding author: kropanevamasha@gmail.com.

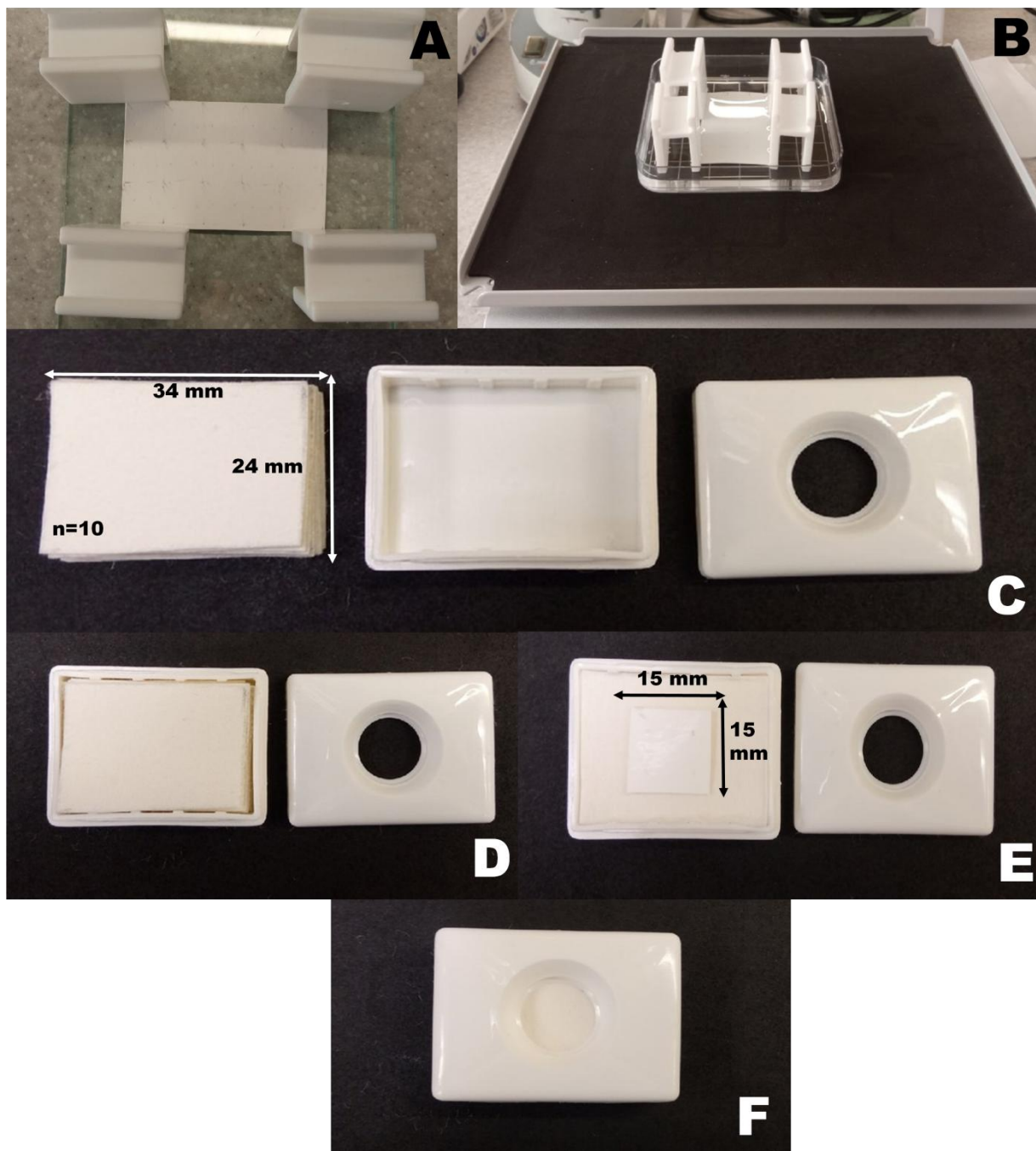


Fig. S1. Fabrication of vertical flow device. A) Drying process of nitrocellulose strip where specific reagents are immobilized ; B) Washing /blocking process of nitrocellulose strip where specific reagents are immobilized; C, D) Disassembled plastic case with an absorbent pad; E) Disassembled vertical flow device with a nitrocellulose strip; F) Vertical flow device ready for use in immunoassay

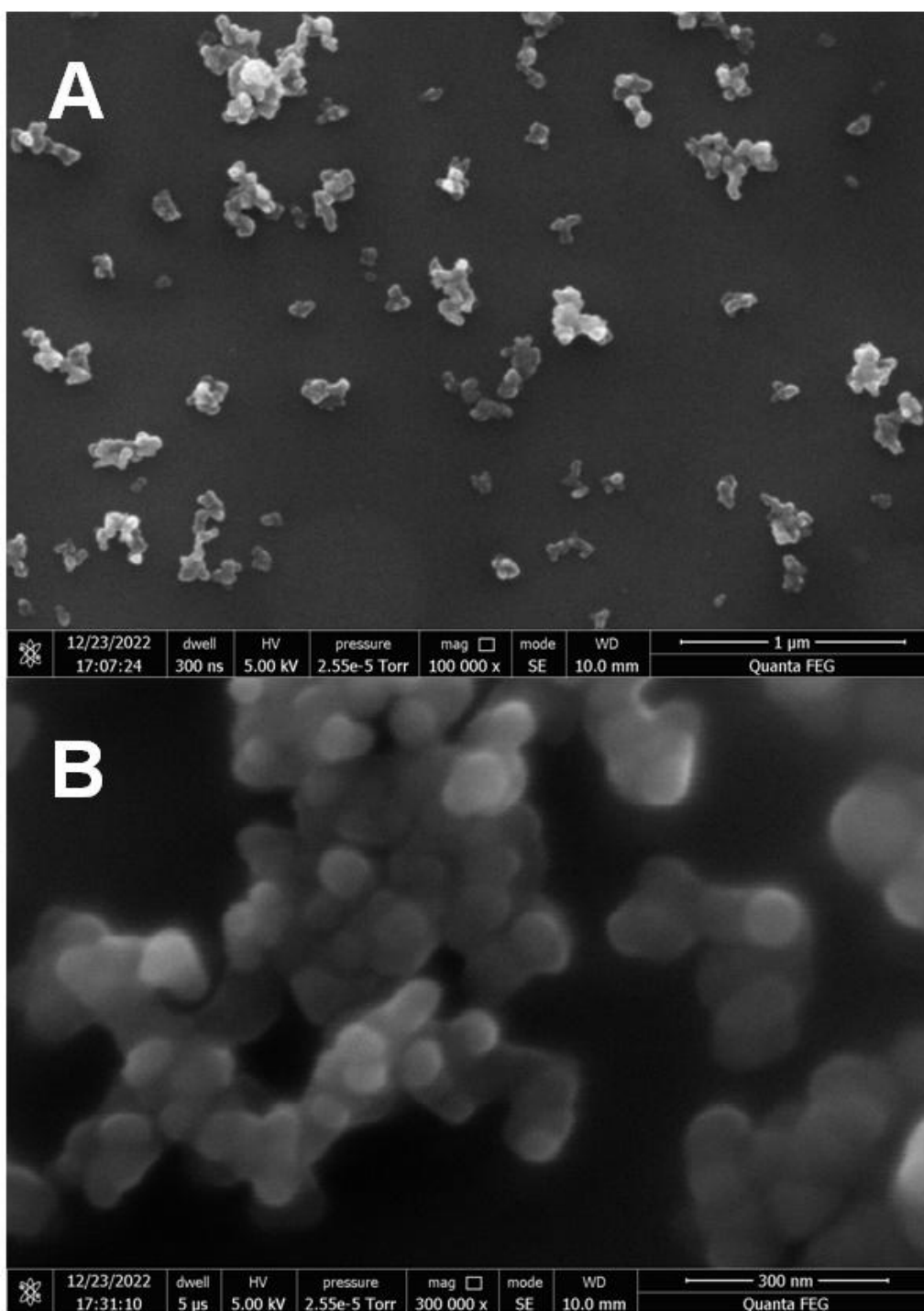


Figure S2. SEM images of CNP@MAb. Scale bar: A-1 μm; B-300 nm

Table S1. Reproducibility of CNP functionalization method

Conjugate number	Mean standard deviation	±	PDI	Concentration, mg/mL
№1	183 27.7		0.17 0.07	3.3
№2	182 15.8		0.19 0.07	3.5
№3	195 39.5		0.17 0.05	4.2

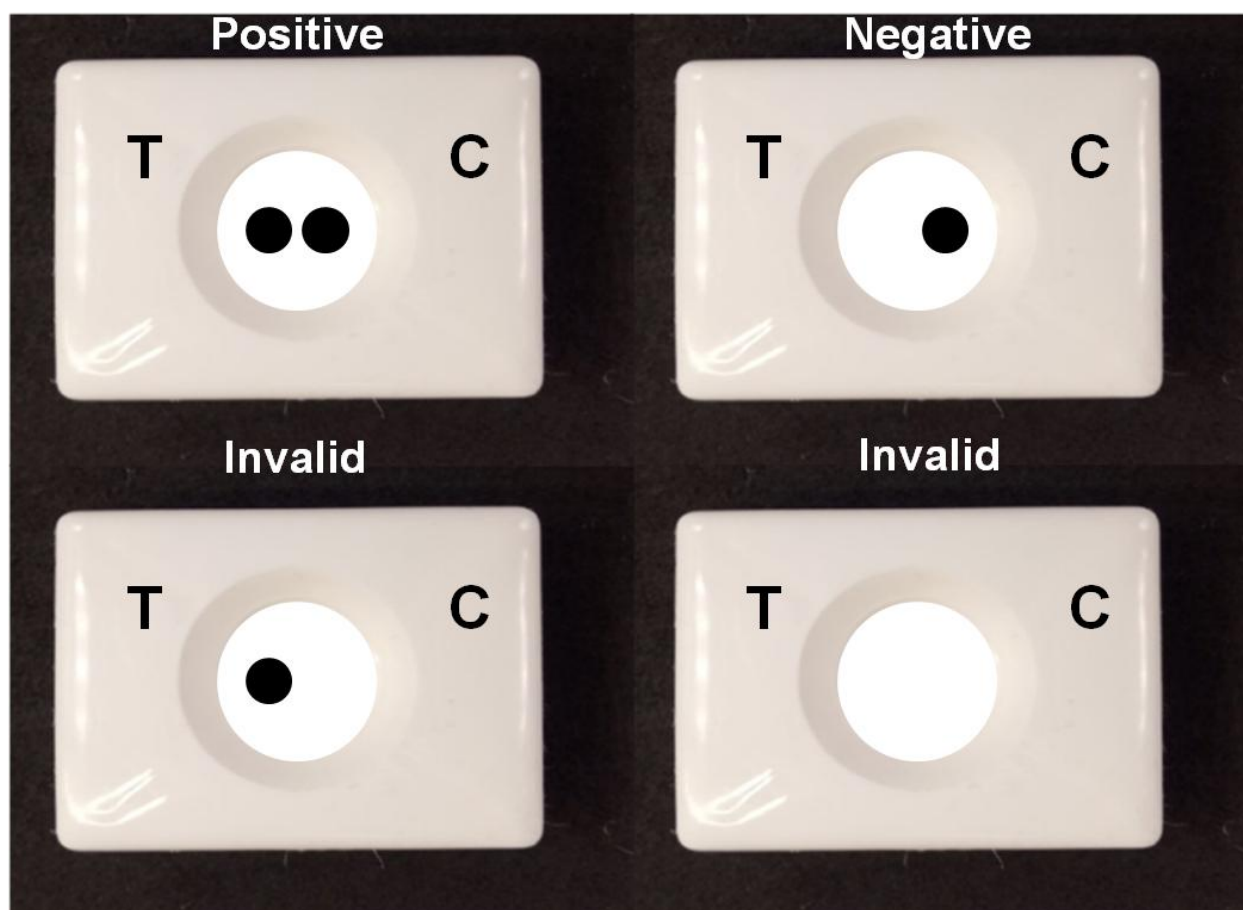


Figure S3. Scheme of assay results interpretation. C-control; T-test.

Table S2. Inter-operator precision

Operator number	Visual assessment	Color intensity, a.u.	CV, %
Positive sample			
1	1	84.03	
2	1	89.9	
3	1	62,7	
4	1	85.2	
5	1	84.3	
6	1	74.9	
7	1	72.5	
8	1	83.65	
Mean± SD		79.54±8.32	10.44
Negative sample			
9	1	7.3	
10	0	-5.8	
11	0	-2.9	
12	0	-4.9	
13	0	-2.2	
14	?	-3.8	
15	0	-1.46	
16	0	0.917	

Quantitative reading of assay results with a flatbed scanner

We used a CanoScan Lide 600f flatbed scanner and CanoScan Toolbox 5.0 (Canon, Japan) to obtain digital images of the vertical flow assay results. To quantify the color of the spots, we have used the software ImageJ (National Institutes of Health, USA). The following scanning parameters were used: mode, grayscale image; resolution, 600 dpi, file format, JPEG. Then the gamma factor of the digital image was corrected in ImageJ to a value of 2 (ImageJ > Process > Math > Gamma). Using “Measure,” we measured the color intensity of the background and spots in arbitrary units (AU) in the range from 255 (black) to 0 (white). Color intensity of the background was measured in 6 replicates and mean value was used. Then we have subtracted the spot intensity from mean background intensity. An example of analytical signal obtaining is shown in Fig S4.

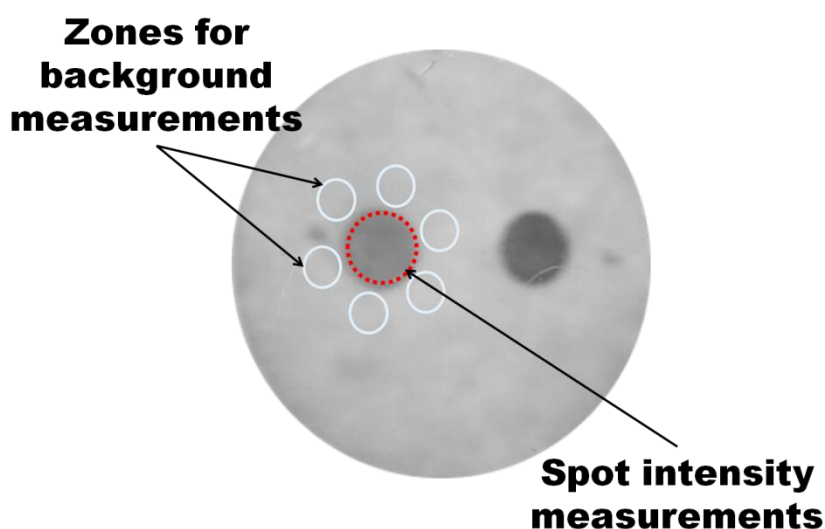


Figure S4. The principle of the obtaining an analytical signal using the ImageJ software